

# Flexible Polymer Substrate and Tungsten Microelectrode Array for an Implantable Neural Recording System

Erin Patrick, Viswanath Sankar, William Rowe, Sheng-Feng Yen, Justin C. Sanchez, and Toshikazu Nishida

**Abstract**—This paper describes the process flow and testing of a substrate for a fully implantable neural recording system. Tungsten microwires are hybrid-packaged on a micromachined flexible polymer substrate forming an intracortical microelectrode array for brain machine interfaces. The microelectrode array is characterized on the bench top and tested *in vivo*. The microelectrode noise floor is less than 2  $\mu\text{V}$  and acute recording results show a signal to noise ratio of 9.9-17.3 dB. The technique of hybrid fabrication of the electrodes on a flexible substrate provides a general platform for the development of an implantable neural recording system

## I. INTRODUCTION

INTRACORTICAL microelectrodes have been used since the 1970s to invasively record action potentials from neurons in the brain. Some of the first published works [1], [2] developed two trends in microelectrode manufacture that still exist today: arrays made from planar micromachining techniques and arrays made with discrete components (micro-wires). Such recording devices have provided the necessary means to communicate with single neurons for therapeutic technologies—i.e. brain machine interfaces (BMIs)—designed for neurologic diseases and injuries [3], [4].

Since the first publications on microelectrodes 40 years ago, the research community has introduced many silicon-based and polymer-based micromachined electrode arrays [5]-[14]. Recently, signal processing and telemetry electronics have been incorporated with the microelectrode array to achieve fully implantable systems [13], [14]. All current efforts are aimed at increasing the efficacy of these recording electrode arrays.

Chronic neuronal recording performance can be improved by floating electrodes that provide strain relief to electrodes and thus minimize tissue damage [15]. Devices best suited to achieve reduced tissue strain use a flexible cable to connect the recording sites to the external connector or circuitry anchored to the skull [16].

However, flexibility comes with trade-offs. Rousche et al. have fabricated flexible polymer substrate microelectrode arrays with thin film recording sites [7]. One drawback to this design is that because of the devices' dimensions and the flexibility of the polymer, the devices are susceptible to buckling during insertion into the tissue and thus incisions

Manuscript received April 7, 2006. This work was supported by a NIH NINDS grant (#NS053561).

Erin Patrick, Sheng-Feng Yen, Viswanath Sankar, William Rowe, and Toshikazu Nishida are with the Department of Electrical and Computer Engineering, University of Florida, Gainesville, FL 32611 USA (e-mail: ee1@ufl.edu, sfyen@cnel.ufl.edu, vsanka1@ufl.edu, wror001@ufl.edu, nishida@ufl.edu).

Justin C. Sanchez is with the Department of Pediatrics, Division of Neurology, University of Florida, Gainesville, FL 32610 USA, (e-mail: jcs77@ufl.edu).

are necessary for them to be implanted. Cheung et al. report a polymer substrate microelectrode that can be implanted without buckling [10]. However, the extreme flexibility of these and other polymer thin-film arrays requires that they be implanted by hand [6], [17], [18], thereby increasing the labor and reducing implant accuracy.

This paper describes a second generation microelectrode based on [19] using insulated tungsten wires as the electrodes. This design furnishes a flexible microelectrode array capable of implantation without buckling that also provides a flat substrate anchored parallel to the skull yielding a platform for future flip-chip bonded electronics. This design is the first step in an effort to develop a fully implantable microelectrode system (Florida Wireless Implantable Recording Electrode (FWIRE)) [20]. The paper will first describe the process flow and then give bench-top impedance, intrinsic noise experimental data, and acute *in vivo* recording statistics.

## II. MICROELECTRODE DESIGN

The prototype tungsten microelectrode array (Fig. 1) consists of three major components: a polymer substrate with encapsulated wiring, tungsten microwires, and nuts used for anchoring and grounding. Rigid 50  $\mu\text{m}$  diameter tungsten micro-wires are attached to the end of a micromachined flexible cable in a 1-D array, allowing for insertion into the neural tissue without buckling. The micro-wires are spaced 250 $\mu\text{m}$  apart as prescribed for decoupled neural recording [21]. Nuts are provided for screws that anchor the device to the skull and supply the reference potential. Incorporating the fasteners yields a secured flat platform for future population of flip-chip bonded electronics. Device dimensions are given in Fig. 1.

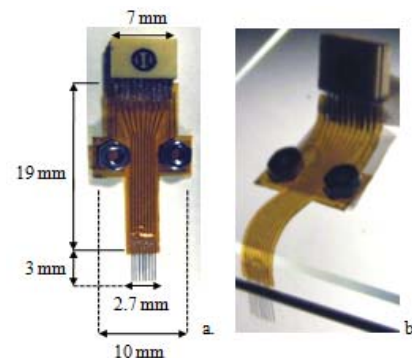


Figure 1. a. Polymer microelectrode array with Omnetics connector. b. Flexibility of microelectrode is shown with assumed *in vivo* position.

### A. Process Flow

The process flow for this electrode was developed based on the process used for the previous generation electrode [19]. Changes were incorporated to improve the quality and reliability of the end product. Aluminum was first sputter deposited on a 4-inch-diameter silicon wafer to a 1  $\mu\text{m}$  thickness as the sacrificial layer. The bottom insulation layer of polyimide (PI 2611, HD Microsystems) was then spin-deposited along with an adhesion promoter (VM 9611, HD Microsystems) and cured at 300  $^{\circ}\text{C}$ . After four spins the resulting thickness was 24  $\mu\text{m}$ . A layer of gold was then sputter deposited to a thickness of 0.1  $\mu\text{m}$ , which was patterned via lift-off to define the wiring and bond pads. Polyimide was next spun five times and cured to achieve a thickness of 30  $\mu\text{m}$ , thereby making the top insulation layer. Chromium was sputter deposited to a thickness of 1000  $\text{\AA}$  and patterned as a hard mask via lift-off. Then an  $\text{O}_2$  reactive ion etch (RIE) was performed to define the device footprint, uncover bondpads and etch grooves for guided placement of the micro-wires. Fifty  $\mu\text{m}$  diameter tungsten wires insulated with polyimide (California Fine Wire) were then placed manually in the etched grooves that formed a jig and electrically connected to the gold wiring of the substrate using a conductive silver epoxy (Epotech). A dicing saw was used to cut the secured micro-wires at a specified length and established a consistent, planar surface for all recording sites. The microelectrode array was then released from the wafer by removing the sacrificial aluminum layer using anodic metal dissolution (constant current in 10% NaCl) as described by [10]. The attachment sites for the tungsten wires and stainless steel nuts were coated with insulating epoxy (Dualbond 707, Cyberbond) and PDMS (Silicone type A, Dow Corning). Lastly, an Omnetics connector was attached to the array with conductive silver epoxy.

## III. RESULTS

### A. Electrical Characterization

#### a. Impedance

A Gamry potentiostat (Series G 300) was used for electrochemical impedance spectroscopy. Individual tungsten recording sites were measured with respect to a large surface area platinum counter electrode and Ag/AgCl reference electrode in 0.9% phosphate buffered NaCl (Sigma) at room temperature. The perturbation voltage was 50 mV. All experimental data were consistent with the Kramers-Kronig relation as prescribed by [22]. The average impedance at 1 kHz for all recording sites is  $50 \pm 10 \text{ k}\Omega$ . This value is characteristic of small surface area electrodes and is on the same order of magnitude as electrodes in the Utah array [8].

Using the equivalent circuit model shown in Figure 2 to describe the electrode/electrolyte interface, the impedance data was regressed giving the reported circuit parameters. These parameters were determined using data in the range of 100 Hz to 10 kHz.

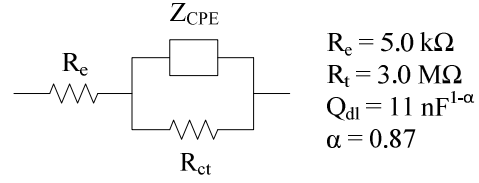


Figure 2. Equivalent circuit for electrode/electrolyte interface.  $R_e$  is the electrolyte resistance,  $R_t$  is the charge transfer resistance and  $Z_{CPE}$  is the double layer constant phase element given by  $Z_{CPE} = [j\omega Q_{dl}]^{-1}$ .

#### b. Noise Floor

Experimental noise data was measured for the tungsten recording sites immersed in phosphate buffered saline at room temperature with reference to an Ag/AgCl electrode at equilibrium. The thermal noise signal from the electrochemical interface was amplified by a low noise voltage amplifier (Stanford Research System (SRS) 560) with gain of 1000 and then recorded with a SRS 785 spectrum analyzer from 1 Hz to 10 kHz.

The thermal noise may be calculated from the real part of the electrode/electrolyte interface impedance as follows

$$V_n(\text{rms}) = \sqrt{4kT \int_{\omega_L}^{\omega_H} \text{Re} \left( R_e + \frac{R_t}{1 + (j\omega)^\alpha Q_{dl} R_t} \right) d\omega}, \text{ where}$$

$\omega_H$  and  $\omega_L$  are the high and low pass-band corner frequencies of the recording amplifier,  $k$  is Boltzmann's constant, and  $T$  is temperature [23]. The theoretical rms noise voltage of the neural probe is 1.27  $\mu\text{V}$  based on the regressed equivalent components in the frequency range of 100 Hz to 6 kHz. The experimental rms noise voltage determined from the noise data is  $1.59 \pm 0.12 \mu\text{V}$  in the same frequency range.

### B. In vivo Characterization

#### a. Surgical Implantation

The flexible electrode arrays were implanted into an adult male Sprague-Dawley rat to test the electrode-substrate configuration and recording performance. All animal procedures have been approved by the University of Florida IACUC. The rats were first anesthetized and the surgical site was thoroughly sterilized. The top of the skull was exposed by a mid sagittal incision between the eyes, and the landmarks bregma, and lambda were located on the skull. A craniotomy was drilled (+1mm anterior to bregma, 2.5mm lateral) at the site corresponding to the forelimb region of the motor cortex [24]. At the site of the electrode implantation, the dura was removed to expose the cortex. The entire assembly was implanted vertically as shown in Fig. 3a and lowered to a depth of 1.66 mm using a micropositioner to minimize distress and damage to the brain tissue. While driving the electrode, electrophysiologic recordings were used to locate pyramidal cell activity in layer V of the cortex. During this procedure, the assembly was observed to be rigid and no buckling was present. Once the electrode

was positioned, it was supported with cranioplastic cement (Plastics-1) attached to a screw placed adjacent to the craniotomy. After the array was secured, the entire assembly was folded down to lay flat against the table of the skull as shown in Fig. 3b. The flexible substrate was then permanently grounded using a second screw.

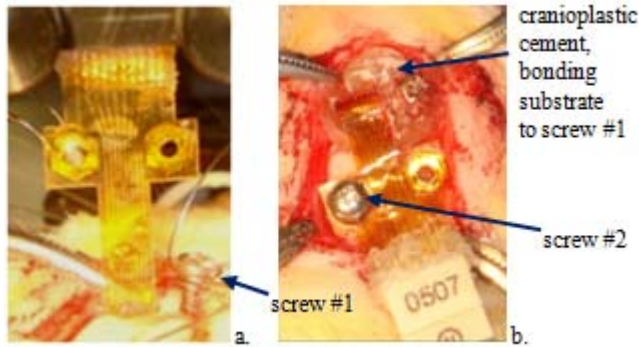


Figure 3. a) Vertical implantation without buckling. b) Final placement of microelectrode secured to skull with screw.

*b. Electrophysiological Recordings*

Neuronal recordings were obtained using a TDT System 3 Real-time Signal Processing System (Tucker-Davis Technologies, Alachua, FL). The headstage was interfaced to the substrate through an Omnetics 18 pin low-profile connector. Extracellular signals were recorded at a sampling rate of 12,207 Hz (16 bits resolution) and bandpass filtered from 500 to 6000 Hz. Data were recorded, digitized and stored on a personal computer for use in offline analysis.

*c. Data Analysis*

Action potentials were discriminated off-line with Spike2 (CED, UK). For each of the eight electrodes, simultaneous recordings lasting 170 seconds were used in the analysis. To detect candidate action potentials, a threshold was applied to the data and a set of templates was formed. Signals with at least a biphasic component within a 1.6-ms window that occurred more than 25 times with similar shape (80%) was categorized as a new neural template. All waveforms that did not match characteristic neural depolarization behavior were considered as noise and removed. The remaining waveforms were sorted according to the amplitude and shape of generated templates, and any waveform templates that were significantly similar to each other were combined into a single template. Principal component analysis (PCA) was used to cluster waveform variance within templates. ISI distribution curves for each neuron in the channels displayed individual Poisson distributions as expected, and showed distinct neurons for each unit waveform.

*d. Electrode Performance*

After the action potential waveforms were properly isolated and sorted, the peak-to-peak amplitude (PPA) was evaluated by computing the average waveform of all spikes belonging to the same neuron. The potential difference was then measured from the apex of the depolarization peak to the apex of the hyperpolarization peak. In addition to the

PPA, the noise floor of each channel was evaluated by computing the root mean square value of all signals excluding recognized neuron waveforms within the channel. The signal-to-noise ratio (SNR) for each neuron was calculated using a ratio of these two values. A representative section of recorded data is shown in Figure 4. Here we can qualitatively see three distinct neuron waveforms with a low noise floor.

The overall performance of the electrode is quantified in terms of neuronal yield, noise floor, peak to peak amplitude, and SNR and is reported in Table 1. A total of 5 waveforms could be extracted from this 8-channel array. The electrodes and recording system performed to discriminate action potential amplitude as high as 30  $\mu\text{V}$  and as low as 12.8  $\mu\text{V}$ . The average RMS noise floor is 3.3  $\mu\text{V}$ . The “pile plots” of action potentials shown in Figure 5 indicate the repeatability of the waveforms.

TABLE I  
NEURAL YIELD FOR MICROELECTRODE ARRAY

Channel	1	7
Yield (neurons)	3	2
Noise Floor ( $\mu\text{V}$ , RMS)	4.1	2.9
Neuron Amplitude ( $\mu\text{V}$ , PtP)	30.0	20.7
	22.3	14.2
	12.8	
SNR(dB)	17.3	17.1
	14.7	13.8
	9.9	

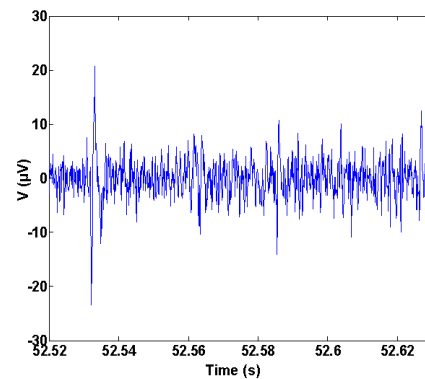


Figure 4. Data from neural recording channel number 1 in the rat motor cortex at a depth of 1.66  $\mu\text{m}$  during implantation surgery.

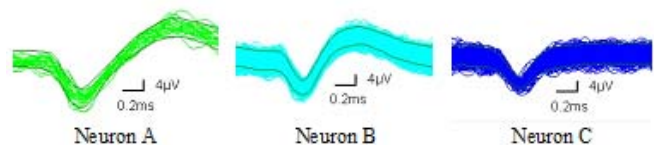


Figure 5. Three distinct neurons extracted during spike sorting in channel number 1 of the recorded data.

#### IV. CONCLUSION

A prototype of a flexible substrate tungsten microelectrode array has been developed and tested for the Florida Wireless Implantable Recording Electrode (FWIRE) project. This design uses discrete tungsten micro-wires as the electrodes in contact with the brain and a flexible polymer substrate designed to lay flat on the skull which provides a base for future designs incorporating flip-chip bonded electronics. Bench-top experiments give an average impedance of 50 k $\Omega$  at 1 kHz and an rms noise floor less than 2  $\mu$ V. Acute recordings show signal to noise ratios as high as 17 dB with a corresponding noise floor of 3.3  $\mu$ V for two channels showing discernable action potentials. Thus, the minimum detectable signal is limited by the recording electronics. In theory, two arrays may be placed parallel to each other and connected to the existing dual row Omnetics connector achieving a (2 by 8 channel) 2-D array. The presented design may be adapted to use more noble micro-wire materials such as platinum or iridium to decrease the risk of surface modification via electrochemical processes with tungsten wires as postulated by [25]. The hybrid manufacturing approach taken with this design allows the microelectrode array to be implanted accurately and without buckling as the micro-wires provide sufficient structural integrity during insertion. Future work will include chronic testing of the microelectrode array.

#### ACKNOWLEDGEMENTS

We thank Dr. Mark Orazem from the Department of Chemical Engineering at the University of Florida for use of the EIS equipment.

#### REFERENCES

- [1] K.D. Wise, "An integrated-circuit approach to extracellular micro-electrodes," *IEEE Trans. Biomed. Eng.*, vol. 17, pp. 238-247, 1970.
- [2] M. Salcman, "Design, fabrication and in-vivo behavior of chronic recording intracortical microelectrodes," *IEEE Trans. Biomed. Eng.*, vol. 20, pp. 253-260, 1973.
- [3] F. A. Mussa-Ivaldi and L. E. Miller, "Brain-machine interfaces: computational demands and clinical needs meet basic neuroscience," *Trends in Neuroscience*, vol. 26, pp. 329-334, 2003.
- [4] R. A. Andersen, et al., "Cognitive neural prosthetics," *Trends in Cognitive Sciences*, vol. 8, pp. 486-493, 2004.
- [5] R. J. Vetter, et al., "Development of a microscale implantable neural interface (MINI) probe system," in *IEEE Engineering in Medicine and Biology 27th Annual Conference Shanghai, China, 2005*, pp. 7341-7344.
- [6] S. Takeuchi, et al., "3D flexible multichannel neural probe array," *Journal of Micromechanics and Microengineering*, vol. 14, pp. 104-107, 2004.
- [7] P. Rousche, et al., "Flexible Polyimide-Based Intracortical Electrode Arrays with Bioactive Capability," *IEEE Trans. Biomed. Eng.*, vol. 48, pp. 361-371, 2001.
- [8] P. Rousche and R. Normann, "Chronic recording capability of the Utah Intracortical Electrode Array in a cat sensory cortex," *Journal of Neuroscience Methods*, vol. 82, pp. 1-15, 1998.
- [9] M. Kindlundh, et al., "A neural probe process enabling variable electrode configurations," *Sensors and Actuators B: Chemical*, vol. 102, pp. 51-58, 2004/9/1 2004.
- [10] K. C. Cheung, et al., "Flexible polyimide microelectrode array for in vivo recordings and current source density analysis," *Biosensors and Bioelectronics*, vol. 22, pp. 1783-1790, 2007.
- [11] K. D. Wise and J. B. Angell, "A microprobe with integrated amplifiers for neurophysiology," in *IEEE International Solid-State circuits Conference*, 1971.
- [12] J. Ji and K. D. Wise, "An implantable CMOS circuit interface for multiplexed microelectrode recording arrays," *IEEE Journal of Solid State Circuits*, vol. 27, pp. 433-443, 1992.
- [13] K. D. Wise, et al., "Wireless Implantable Microsystems: High Density Electronic Interfaces to the Nervous System," *Proceedings of the IEEE*, vol. 92, 2004.
- [14] R. R. Harrison, et al., "A Low-Power Integrated Circuit for a Wireless 100-Electrode Neural Recording System," *Solid-State Circuits, IEEE Journal of*, vol. 42, pp. 123-133, 2007.
- [15] R. Biran, et al., "The brain tissue response to implanted silicon microelectrode arrays is increased when the device is tethered to the skull," *Journal of Biomedical Materials Research Part A*, vol. 82, pp. 169-178, 2007.
- [16] J. Hetke, et al., "Silicon ribbon cables for chronically implantable microelectrode arrays," *IEEE Trans. Biomed. Eng.*, vol. 41, pp. 314-321, 1994.
- [17] T. Suzuki, et al., "Flexible neural probes with micro-fluidic channels for stable interface with the nervous system," in *Proceedings of the 26th Annual International Conference of the IEEE EMBS*, 2004.
- [18] Y. Yao, et al., "Silicon microelectrodes with flexible integrated cables for neural implant applications," in *IEEE EMBS Conference on Neural Engineering Kohala Coast, Hawaii, USA, 2007*.
- [19] E. Patrick, et al., "Design and Fabrication of a Flexible Substrate Microelectrode Array for Brain Machine Interfaces," *EMBS '06. 28th Annual International Conference of the IEEE*, 2006, pp. 2966-2969.
- [20] R. Bashirullah, et al., "Florida wireless implantable recording electrodes (FWIRE) for brain machine interfaces," in *IEEE International Symposium on Circuits and Systems New Orleans, LA, USA, 2007*.
- [21] K. L. Drake, et al., "Performance of planar multisite microprobes in recording extracellular single-unit intracortical activity," *IEEE Trans. Biomed. Eng.*, vol. 35, pp. 719-732, 1988.
- [22] M. Orazem, "A systematic approach toward error structure identification for impedance spectroscopy," *J. Electroanalytical Chemistry*, vol. 572, pp. 317-327, 2004.
- [23] M. Stecker and T. Patterson, "Electrode impedance in neurophysiologic recordings: 1. Theroy and intrinsic contributions to noise," *Am. J. END Technol.*, vol. 38, pp. 174-198, 1998.
- [24] G. Paxinos, *The rat brain in stereotaxic coordinates*. Sydney: Academic Press, 1997.
- [25] J. C. Sanchez, et al., "Structural modifications in chronic micro-wire electrodes for cortical neuroprosthetics: A case study," *IEEE Trans. on Neural Syst. And Rehab. Eng.*, vol. 14, pp. 217-221, 2006.